# SOTERIA MIDTERM WORKSHOP

## IMPROVEMENT OF THE PHYSICALLY-BASED CONSTITUTIVE STRESS-STRAIN EQUATIONS AND THE POST-IRRADIATION FRACTURE RESPONSE OF RPV STEELS

## 10TH APRIL 2018

Contribution to SOTERIA WP5
Co-workers: B. Marini, P. Forget, K. Singh, L. Vincent, Y. Li
Speaker: **Christian Robertson**

Long-term goal or vision: predicting dose-dependent fracture toughness response based on non-destructive post-irradiation examinations (material polycrystalline microstructures, i.e. grain sizes and orientations; irradiation defect microstructures ) and physically based models
☞minimizing/optimizing time-consuming/costly mechanical testing of post-irradiated specimens in hot cells

# Cross-cutting WP2/WP3/WP5 issue

Thick-walled components: microstructure and fracture toughness variability

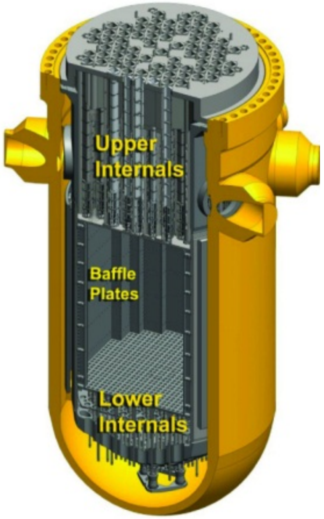

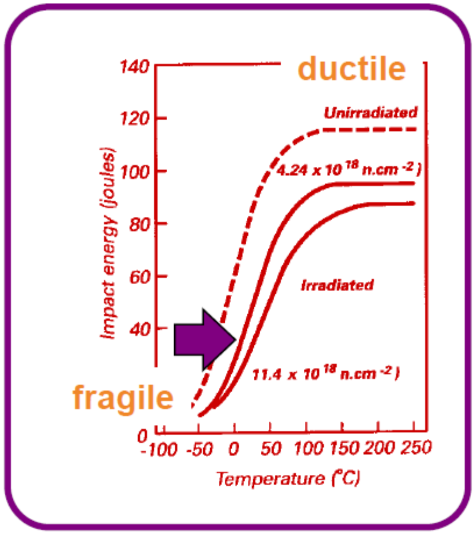

Microstructural variations = one possible contribution…

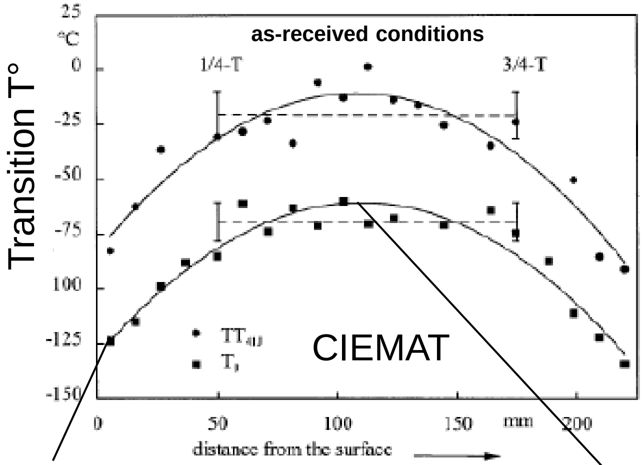

CIEMAT

B. Marini, Lecture series

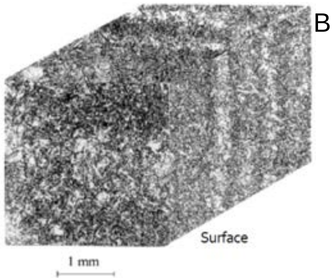

outer surface

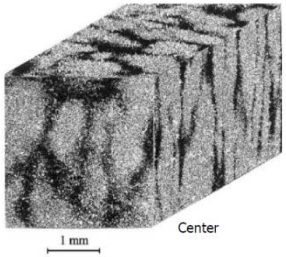

center

☞Modelling efforts adressing: dose-dependent fracture response and its scattering

# «Local approach of fracture models»

- $\Sigma$ : specimen-scale loading level
- $V_0$ : representative elementary volume
- $\sigma$ : stress level acting on $V_0$

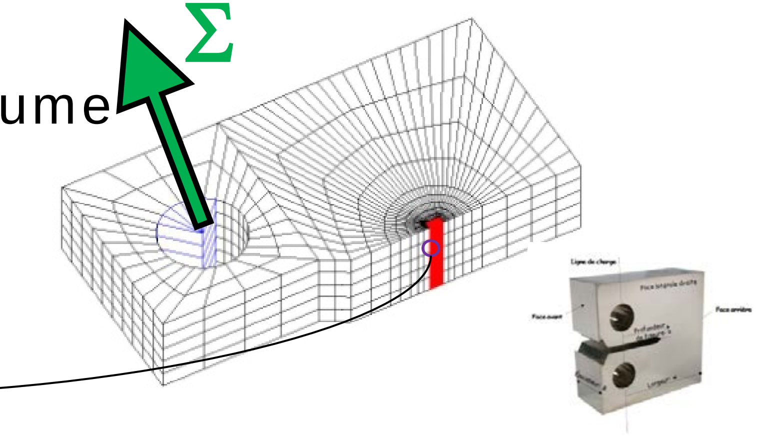

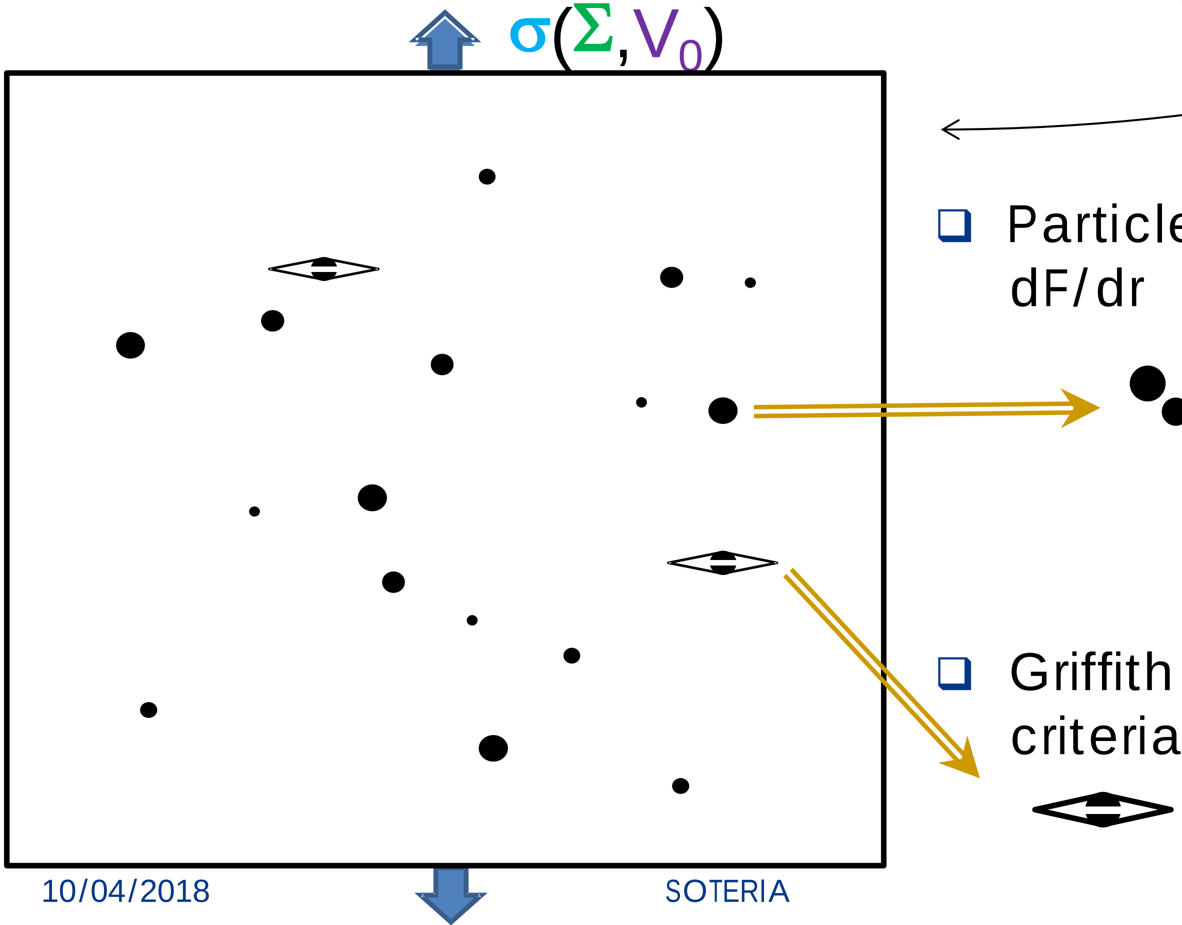

- Particle size distribution: f(r) = dF/dr

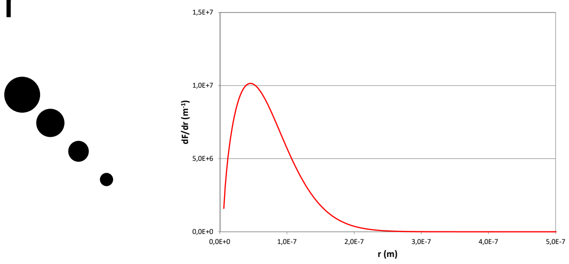

- Griffith fracture propagation criteria :

$$\sigma_c = \sqrt{\frac{\pi}{2(1-\nu^2)} \cdot \frac{E \cdot \gamma_f}{r}}$$

# ...including local stress distribution (MIBF)

➢ **MIBF model INPUTS** : irradiation-induced hardening level, particle size distribution, surface energy, grain-size, grain orientation, grain-scale stress fields

J. Nucl. Mat. 406 (2010) 91-96

RPV steel microstructure

⇒ local stress distribution $\sigma^*$ inside $V_0$.

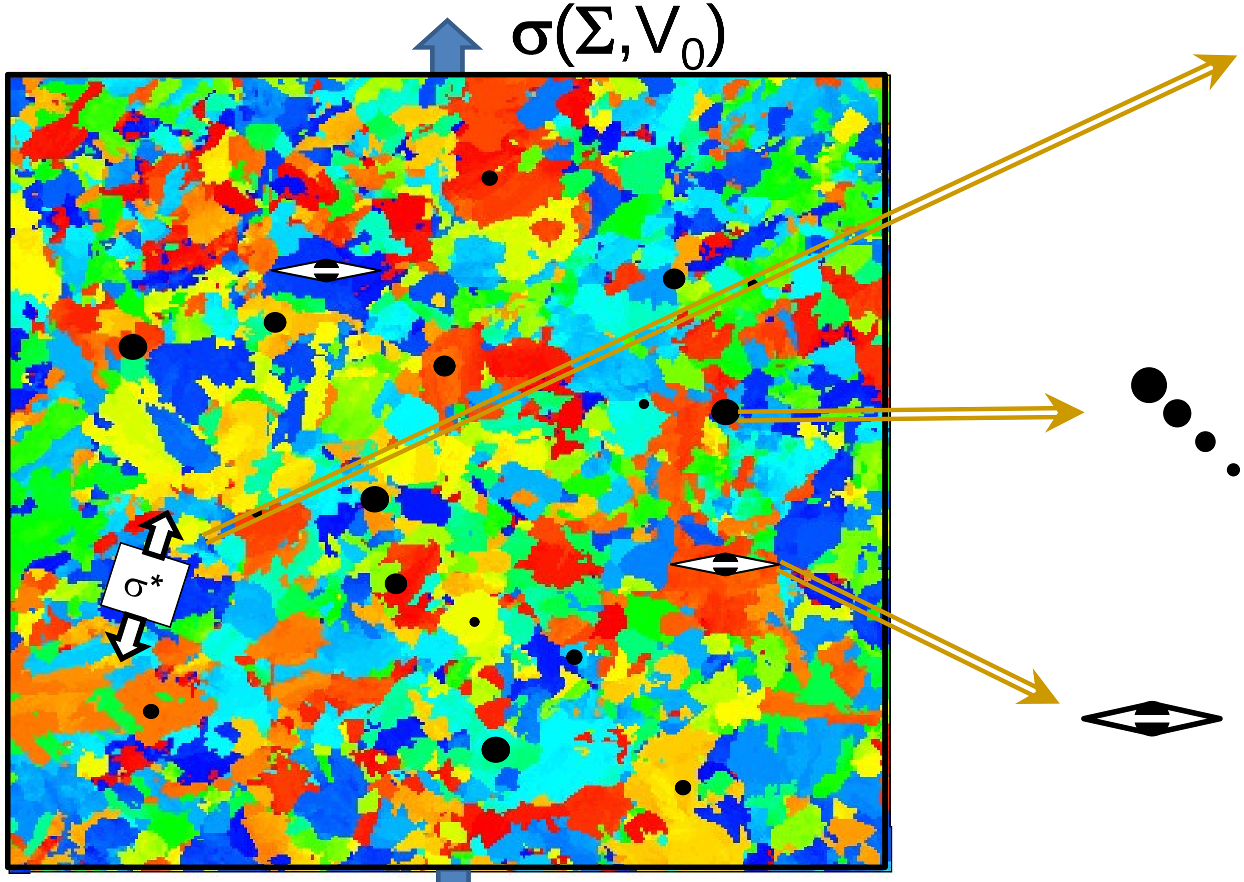

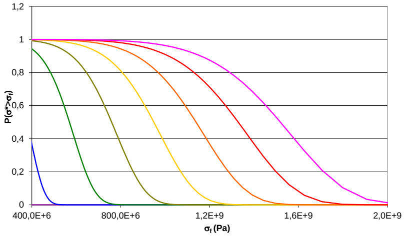

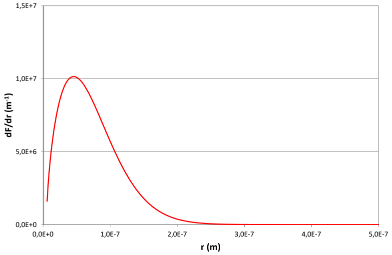

$$\sigma_c = \sqrt{\frac{\pi}{2(1-\nu^2)} \cdot \frac{E \cdot \gamma_f}{r}}$$

# Weakest link assumption

Cracked inclusion: brittle fracture initiator

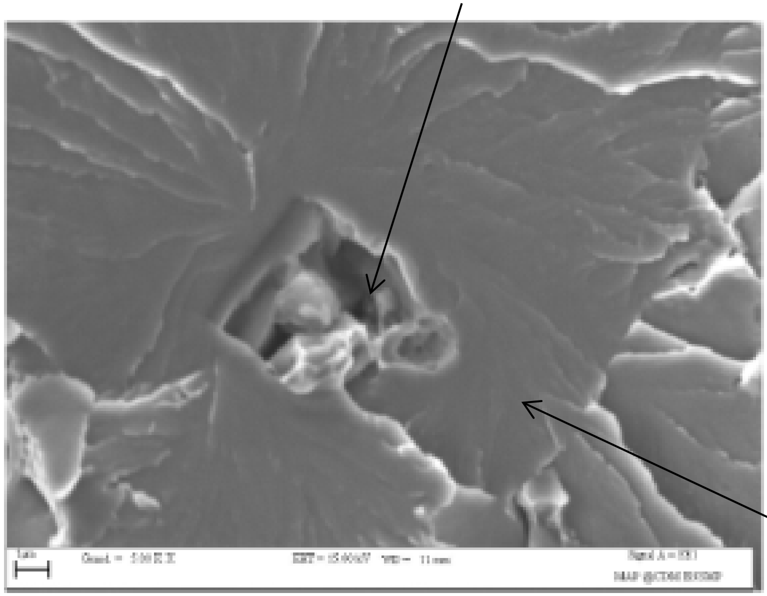

Cleavage fracture surface

Weakest leak assumption

I- all inclusions/particles break down, for $\varepsilon > \varepsilon_{p0}$
II- micro-cracks grow (or not) according to a definite criteria
III- first micro-crack develops → the whole specimen fails

IV- **fracture toughness then directly relates to plastic zone size $a_0$, near the micro-crack initiators**

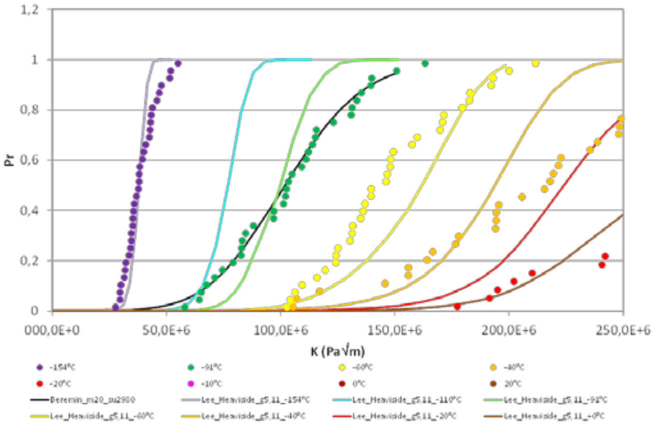

Transition curves, DBT shift

# Micro-crack induced plastic zone?

Q. Effect of straining temperature on $a_0$?
Q. Grain size and orientation effect on $a_0$?
Q. Dose effect, irradiation temperature effect, on $a_0$?

## R. Crack-induced plasticity: dislocation-mediated

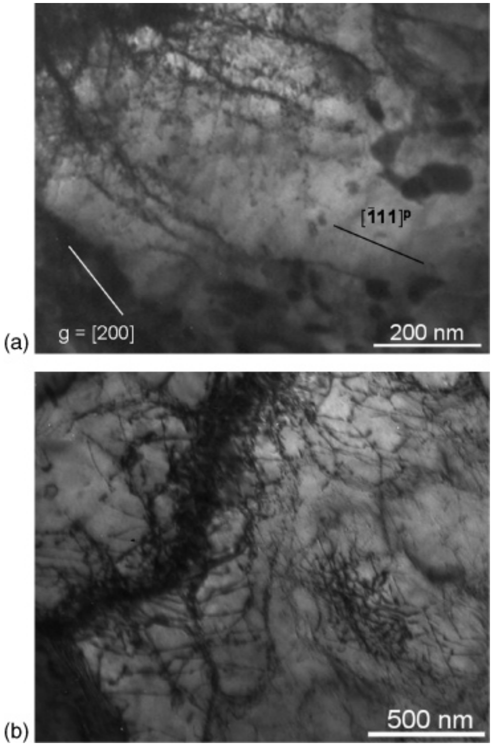

Modelling Simul. Mater. Sci. Eng. **18** (2010) 025003

☞ **«Statistical, investigation of post-irradiation plasticity mechanisms using, 3D DD simulations»**

☞Dislocation Dynamics simulations?

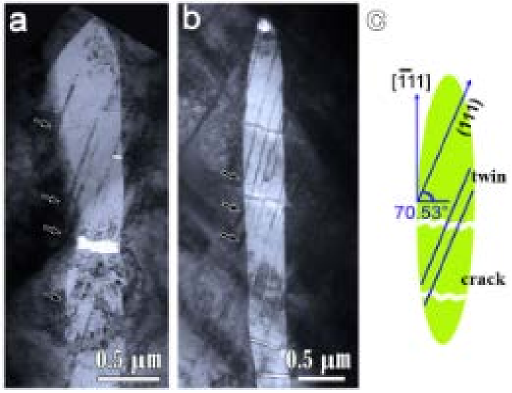

MnS in steel, Sci. Reports 4, 5118 (2014)

# Dislocation dynamics simulations?

« TRIDIS » code

Model. Simul. Mater. Sci. Eng. 6 (1998) 755-770

*Dislocation Model*

Discrete dislocation lines

Discrete time steps: $10^{-10}$ s

Discrete bcc lattice

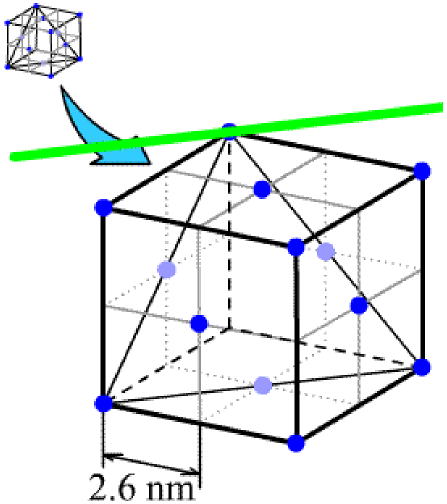

*Stress* → **D**islocation **D**ynamics code

→ Dislocation microstructures

→ Plastic strain

**Dislocation theory**

→ Dislocation mobility (stress and T° dependent)

→ Interaction with radiation defects, other dislocations, GB…

→ Cross-slip

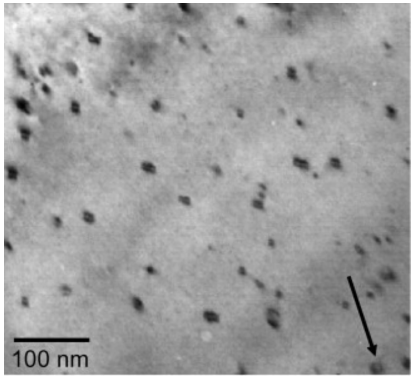

# Dislocation stress-velocity response

## **FCC models** (Cu, FCC Fe)

### **Screw ~ Edge**

Negligible Peierls barrier ($\tau_p$~10 MPa)

**Phonon-drag** mechanism

$$v_{screw}(\tau) = v_{edge}(\tau) = \frac{\tau b}{B}$$

- $\tau$ : applied stress >> $\tau_p$
- $B$ : Viscous drag coefficient
- $b$ : Burgers vector module
- $\tau_p$ : Peierls Stress

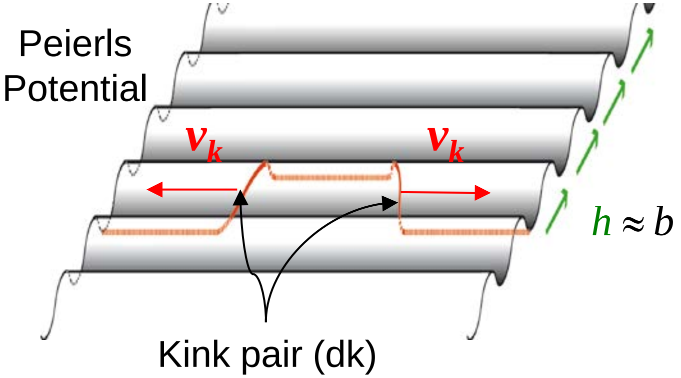

## **BCC Fe and Fe alloys**

### **Screw ≠ Edge**

Velocity anisotropy depends on T°

| Low temperature | High temperature |
|---|---|
| Significant Peierls barrier ($\tau_p$~1GPa)<br>**Thermally activated** mobility<br>$v_{screw}(\tau, T)$ **<<** $v_{edge}(\tau) = \frac{\tau b}{B}$ | **Athermal** regime<br>$v_{screw} \approx v_{edge}$ |

### Low-T screw dislocation mobility mechanism

- **Nucleation** of a kink pairs (thermally activated)
- Kink pair **propagation** $v_k \propto \tau$ « effective » $B_k < B_{edge}$

# Dislocation mobility rules for RPV steels

*Journal of Nuclear Materials* 504 (2018) 84-93

$$v_{screw} = \boldsymbol{hJX'}$$

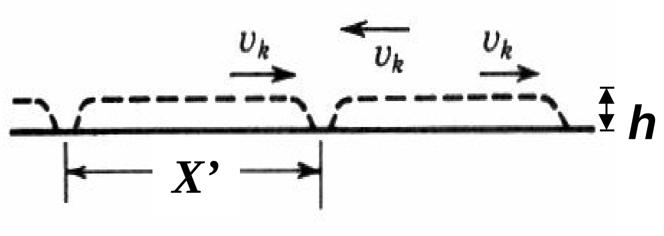

- $\boldsymbol{h}$ : distance between Peierls valleys
- $\boldsymbol{J}$ **[m$^{-1}$s$^{-1}$]** : kink pair **nucleation rate** per unit length
- $\boldsymbol{X'}$ **[m]** : kp **mean free path** before annihilation with another dk [increases with kink velocity ($\boldsymbol{v_k}$) and decreases with $\boldsymbol{J}$]

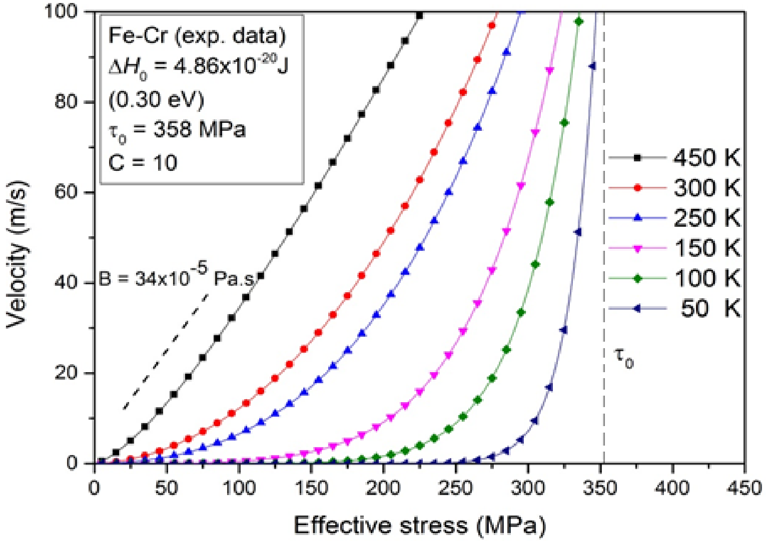

$$v_{screw}(\tau^*, T) = \underbrace{\frac{8\pi b(\tau^*)^2}{\mu B h}}_{\text{Stress-dependent pre-factor}} X' \exp\left(-\frac{\Delta G(\tau^*,T)}{k_B T}\right)$$

☞ **Progressive transition from Low-*T* to Room-*T***

# DD simulation setup

## 1µm$^3$ ferritic grains (Fe-C or Fe-Cr):

- ➢ Defect number density and defect size depend on selected dose and $T_{irr}$ condition
- ➢ Uni-axial tension, strain-rate controlled conditions, fixed straining T°, presence of cross-slip

➢ **Model INPUTS** : grain size, kink-pair activation energy, phonon drag coefficient, irradiation defect size, and number density

❶ Defect-free

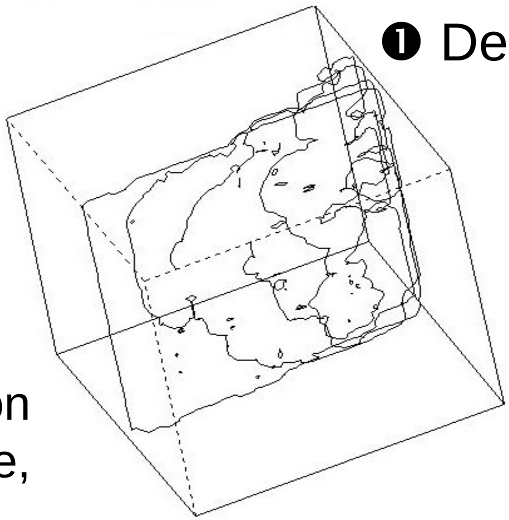

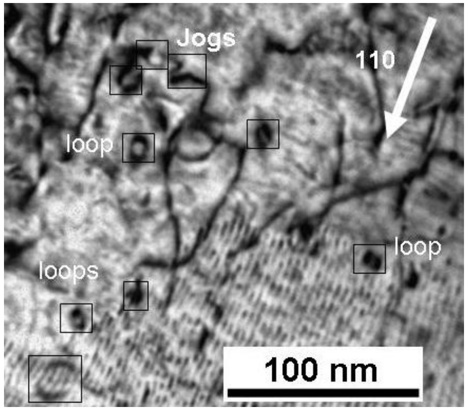

$T_{irr}$=400°C, dose = 1 dpa, defect size D = 50 nm

❷ Irradiated

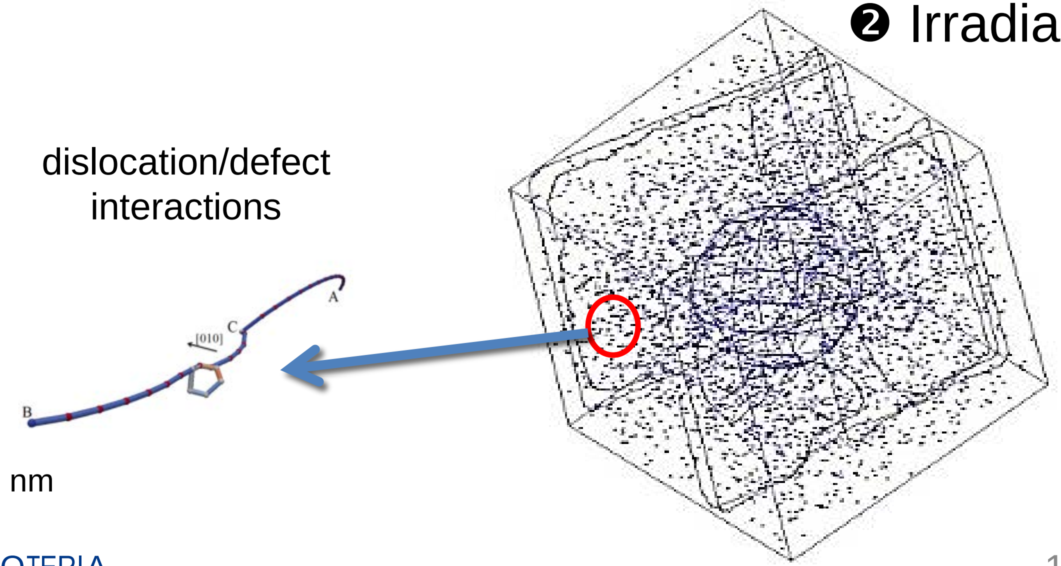

# Predicted defect-induced evolutions

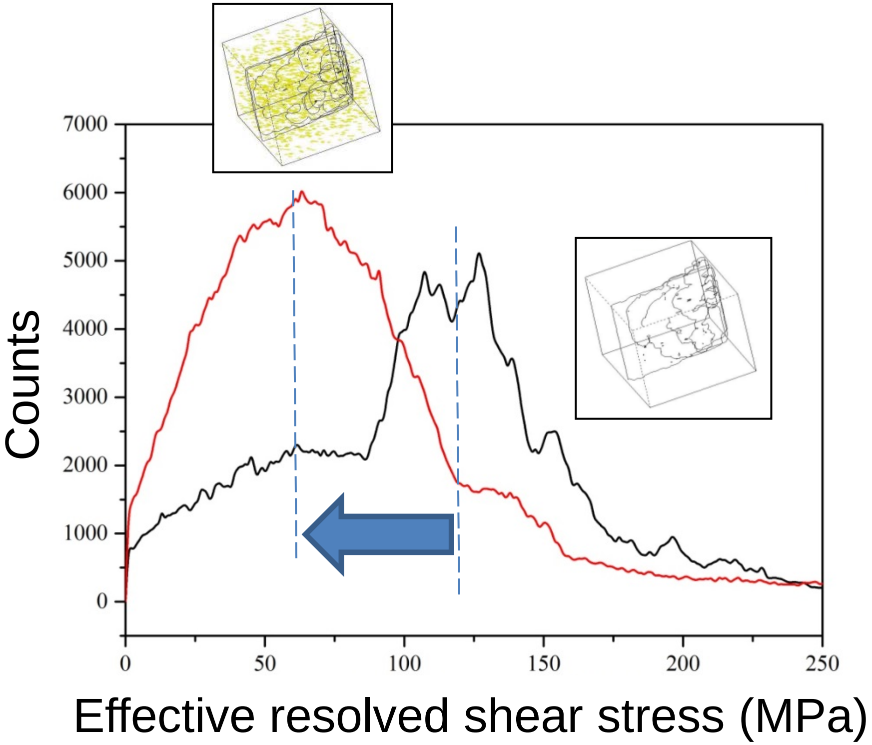

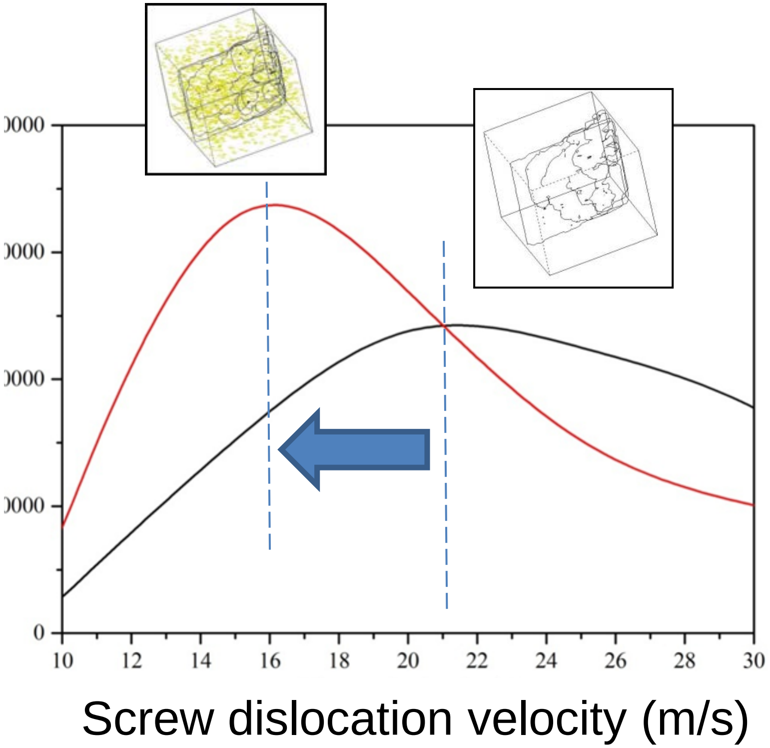

- ➢ Defect-induced effect on effective screw dislocation mobility : **statistically significant**

# DIAT shift: interpretation

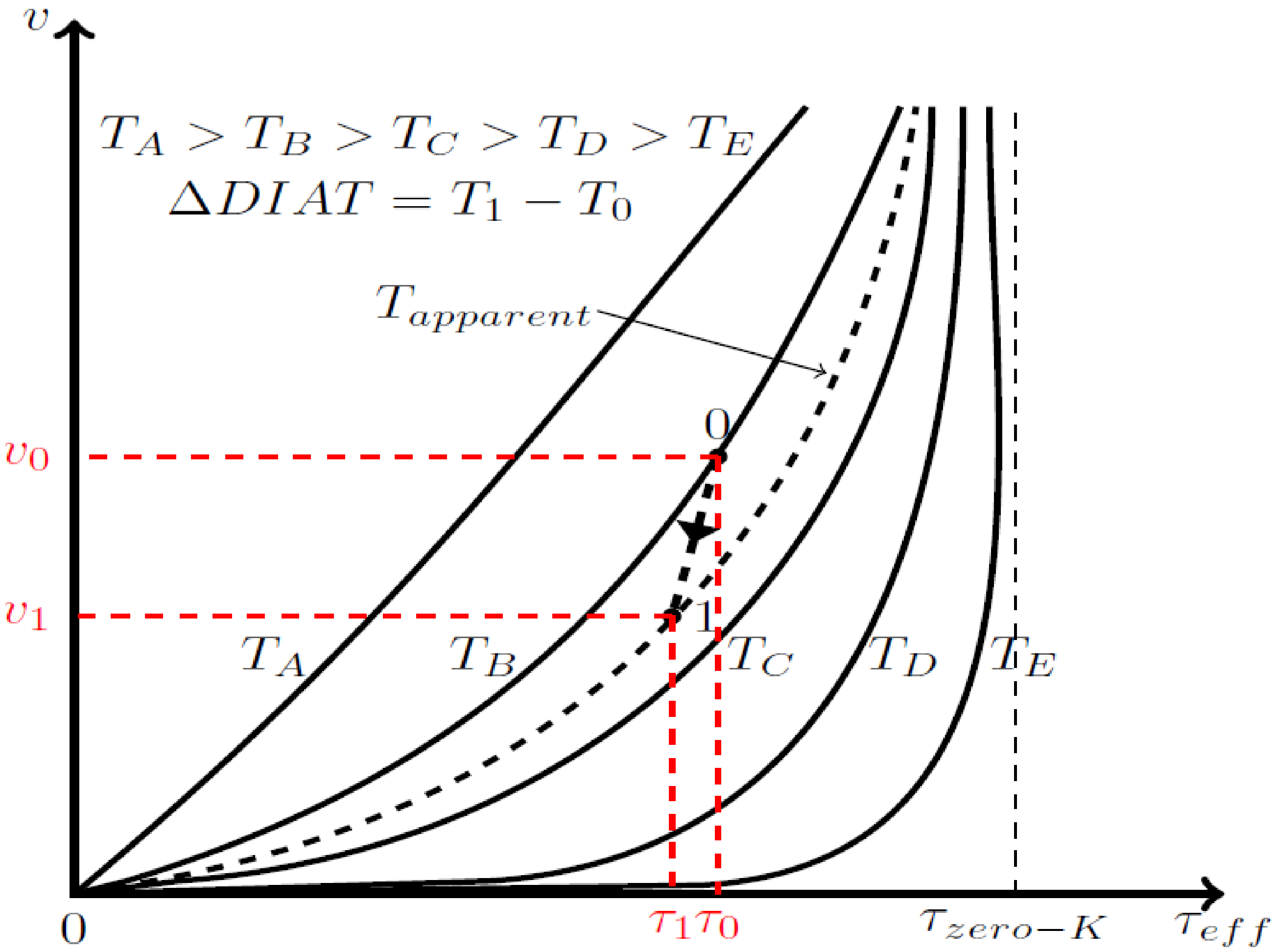

$T_{apparent} - T_0$ = Defect-Induced Apparent straining Temperature shift (ΔDIAT)

# ΔDIAT: a systematical investigation

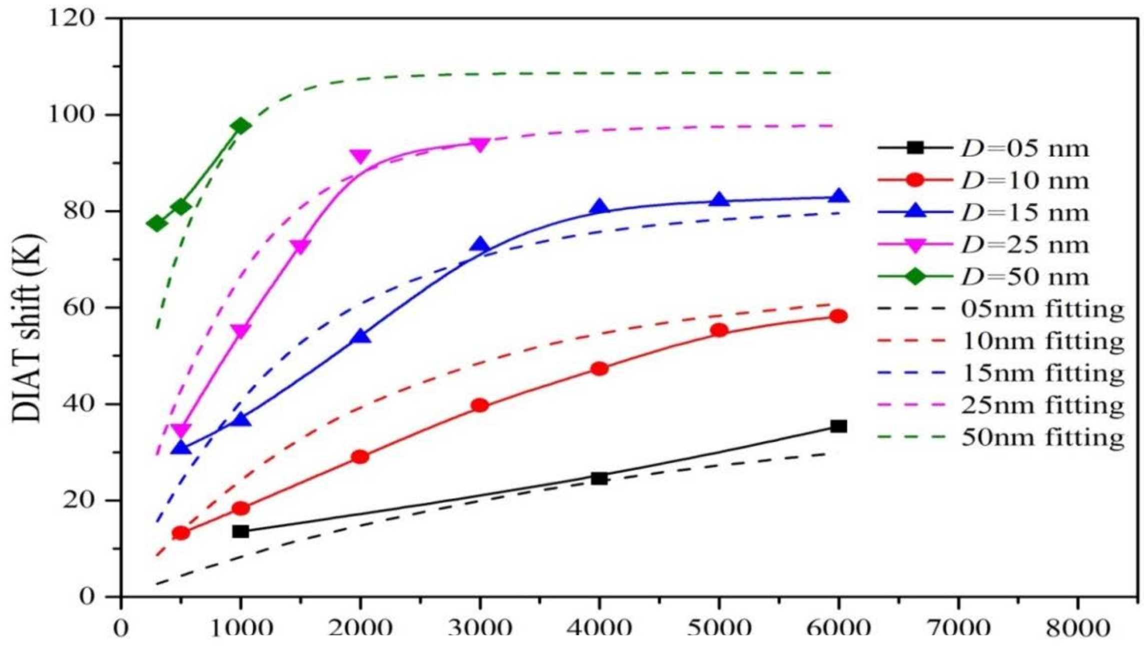

Defect number density $\times 10^{18}$ m$^{-3}$

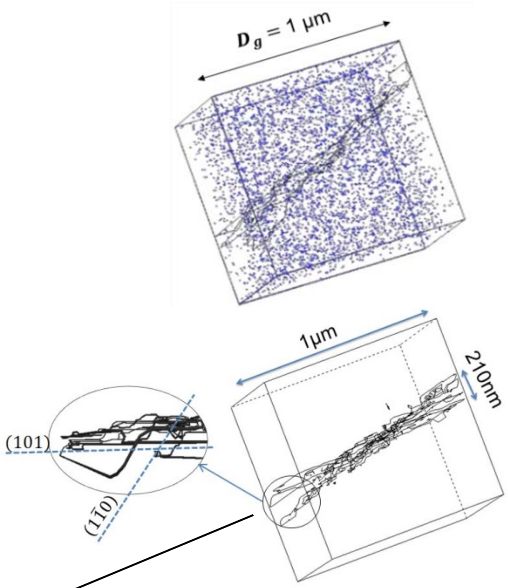

$$\Delta\text{DIAT} = \Delta T_{max}\left(1 - exp\left(-\frac{D}{\lambda}\right)\right)\left(1 - exp(-\boldsymbol{d}^2 DN)\right) \approx \Delta\text{T}_0 \,/\, \Delta\text{DBTT}$$

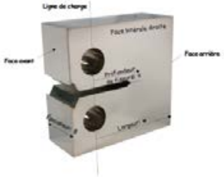

$N$: defect number density (in nm$^{-3}$ ); $D$: defect size (in nm);
and **3 material-dependent scaling parameters** ($\Delta T_{max}$, $d$ and $\lambda$)

This description potentially includes segregation effects at dislocation sources (augmenting $\Delta T_{max}$) and GB (decreasing critical stress-localisation threshold → shear band thickness $d$ and mean free path $\lambda$)

# ΔDIAT/ΔDBTT comparison

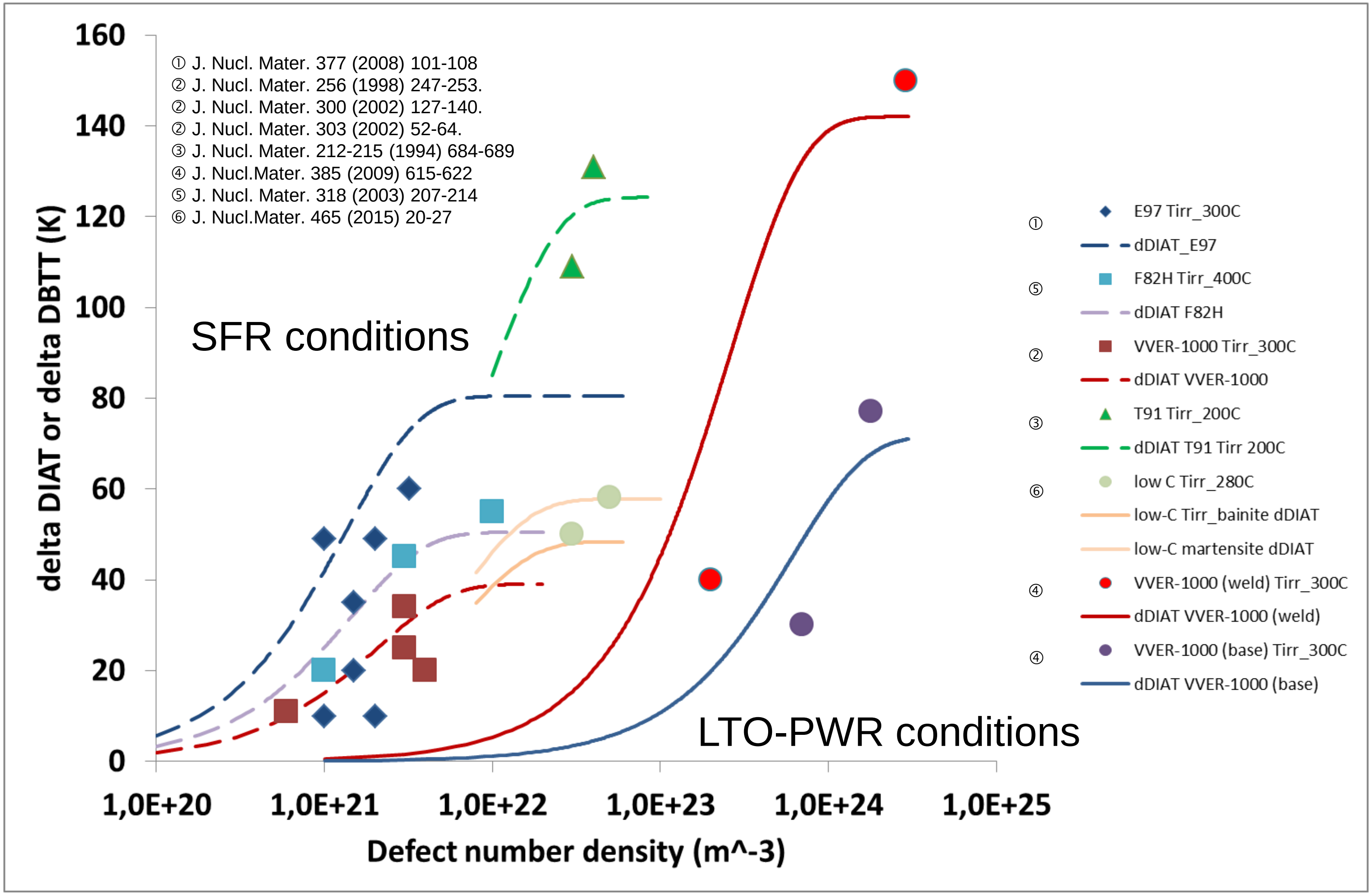

① J. Nucl. Mater. 377 (2008) 101-108
② J. Nucl. Mater. 256 (1998) 247-253.
② J. Nucl. Mater. 300 (2002) 127-140.
② J. Nucl. Mater. 303 (2002) 52-64.
③ J. Nucl. Mater. 212-215 (1994) 684-689
④ J. Nucl.Mater. 385 (2009) 615-622
⑤ J. Nucl. Mater. 318 (2003) 207-214
⑥ J. Nucl.Mater. 465 (2015) 20-27

- ΔDIAT ≈ ΔDBTT [irradiation conditions: little or no segregation at fracture initiators (particles or GB)]
- Absolute toughness levels: link with local approach of fracture/MIBF approach/models
- Support/link dose-dependent crystal plasticity…

# Crystal plasticity approach

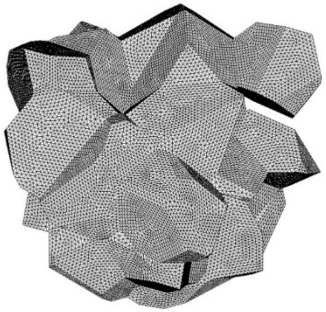

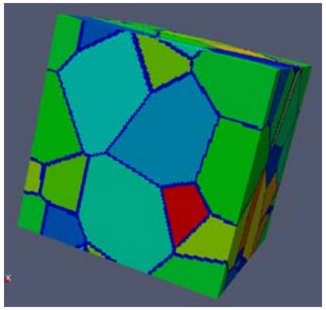

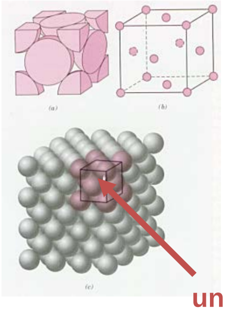

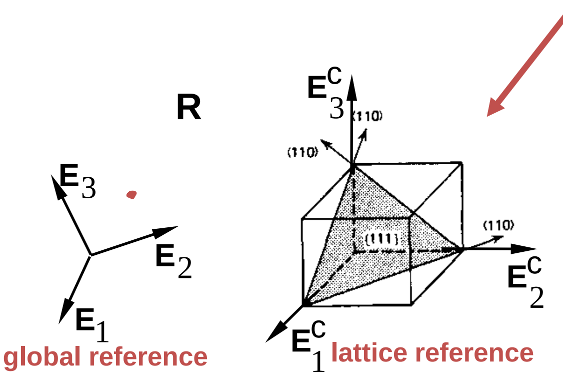

global reference frame

lattice reference frame

**FCC**
**12 slip systems**
**m={111}, s=<110>**

**BCC**
**12 slip systems**
**m={110}, s=<111>**

- ➢ Explicitly models discrete grains and slip systems, accounting for anisotropy of single crystal properties and crystallographic texture.

- ➢ Slip system level constitutive equations for dislocations with use of Internal state variables for various parameters at each slip system

- ➢ Approach used to study aggregate of crystals to obtain a better understanding of single-crystal or poly-crystal behavior.

**Support from DD-based simulations**

- ➢ Physically based stress-velocity rules, system-system interaction strength

- ➢ Evolution of irradiation defect population with increasing strain, mobile dislocation density evolution

# Modified T°-dependent mobility rule

$$\frac{1}{\dot{\gamma}_{total}} = \frac{1}{\dot{\gamma}_{nuc}} + \frac{1}{\dot{\gamma}_{prop}}$$

$$\dot{\gamma}_{nuc} = \rho_{mob} b \frac{8\pi\tau_{eff}^2}{\mu B} exp\left[ -\frac{\Delta H_0}{k_B T}\left(1 - \left[\frac{\tau_{eff}}{\tau_0}\right]^p\right)^q \right] l_s$$

(1)

$\dot{\gamma}_{nuc}$ accounts for thermally activated kink pair nucleation.

The stress-independent $l_s$ term assumes that each nucleated kink-pair sweeps the whole dislocation line, while a given screw dislocation moves from one Peierls valley to the next one.

Inverse of strain rate sensitivity parameter

Reference shear strain rate

$$\dot{\gamma}_{prop1} = \dot{\gamma}_0 \left(\frac{\tau_{RSS}}{\tau_c}\right)^n$$

Requirement of very high value of n = 100 limits its numerical implementation. Generally lower values of n=50 is used to avoid numerical issues.

Use of lower value of n leads to inaccurate coupling between the rate sensitive macroscopic response and rate sensitive evolution of critical shear stress.

$$\dot{\gamma}_{total} \propto \frac{l_s X_\infty}{l_s + X_\infty}$$

$$\dot{\gamma}_{prop2} = \rho_{mob} b \frac{8\pi\tau_{eff}^2}{\mu B} exp\left[ -\frac{\Delta H_0}{k_B T}\left(1 - \left[\frac{\tau_{eff}}{\tau_0}\right]^p\right)^q \right] X_\infty$$

(2)

$$X_\infty = 2\sqrt{\frac{v_k}{J}}$$

Formulations (1)&(2) yield comparable results at the strain rate $10^{-4}$ for $\Delta H_0 > 0.6$ eV.

However, formulation (2) is able to handle a **larger range of strain rate and material parameters**.It is also found to be more robust in terms of convergence in finite element formulation.

# Modified dislocation/defect interaction rule

- ➢ Irradiation defects (assumed to be uniformly distributed) are accounted as obstacles cutting the dislocation glide planes hence treated as forest obstacles to the glide of dislocations.

$$\alpha^{A} = \sqrt{\sum \alpha^{AF} \frac{\rho^{F}}{\rho^{A}_{obs}}}$$

- ➢ Irradiation defects with their density $\rho_{irr} = N_{irr} d_{irr}$ and respective strength interacts with dislocations.

- ➢ Dose level controls the number of loops formed and temperature controls the size of the loop.

Irradiation defect density evolution $$\dot{\rho}_{irr} = -\xi \rho_{irr} \dot{\gamma}$$

Affects $\tau_{eff}$ in eq. (2)

**ξ : loop annihilation parameter**

This term is defect number density dependent (irradiation dose)

# Modified dislocation/defect interaction rule

Through DD simulations → significant dose-dependent increase in total and mobile dislocation density.

This increase is ascribed to interaction of screw dislocations with irradiation defects → dislocation pinning, multiplication.

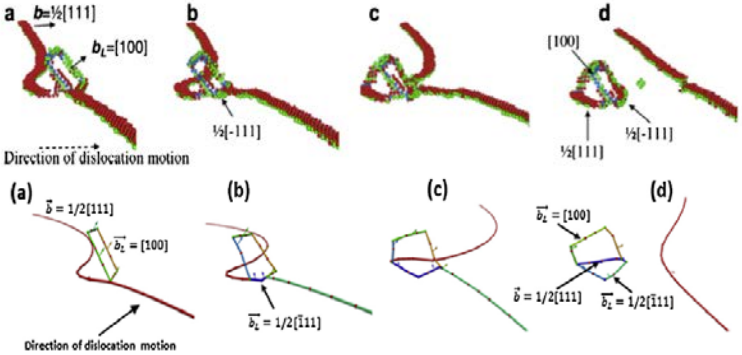

X.J. Shi et al. *J. Nucl. Mat.* 460 (2015) 37-43

$$\dot{\rho_m} = \frac{\kappa\xi}{r_0}\rho_{irr(t)}\dot{\gamma}$$

affects gamma-dot in eq. (2)

☞Interaction means dislocation pinning, which subsequently act as source of mobile dislocation for their further generation.
☞This mechanism/term is defect-size dependent (irradiation temperature)

# Preliminary results: FEM model

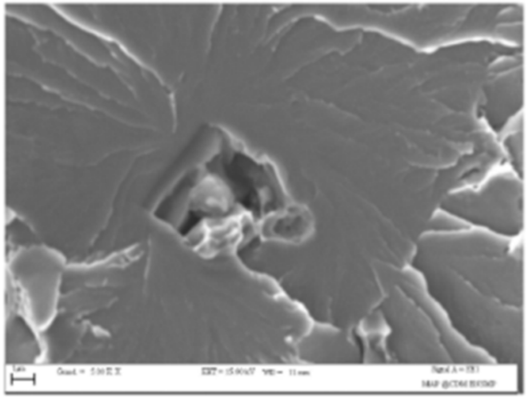

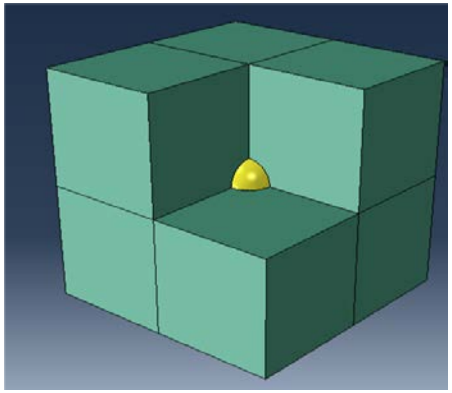

To predict stress field near fracture initiator and its dose-dependent evolutions

☞ Link with DD calculations: ΔDIAT prediciton
☞ Link with MIBF model

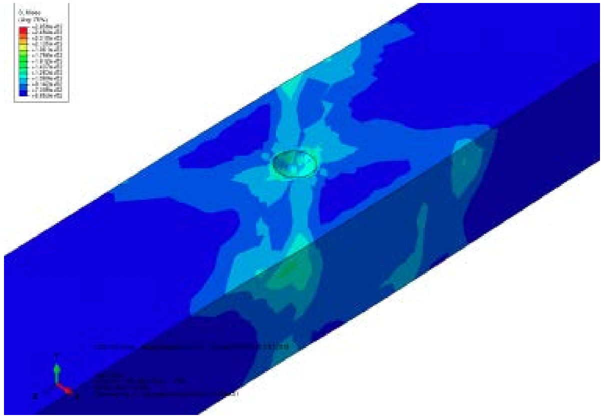

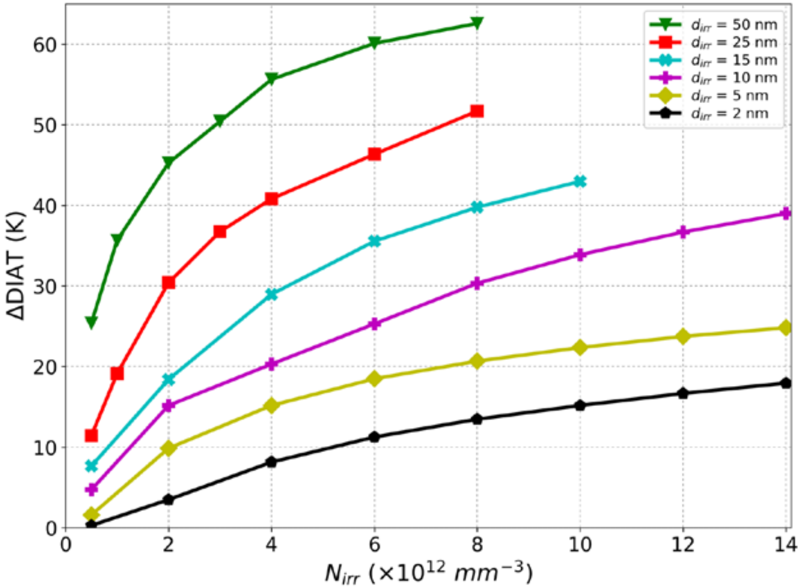

# Preliminary results: dose-dependent stresses

Stress field near fracture initiator:
Weibull statistics description

$$f(\tau_{eff}) = \frac{\beta}{\eta}\left(\frac{\tau_{eff}-\gamma}{\eta}\right)^{\beta-1} exp^{-\left(\frac{\tau_{eff}-\gamma}{\eta}\right)^{\beta}}$$

Scale Parameter

Shape Parameter

Position Parameter

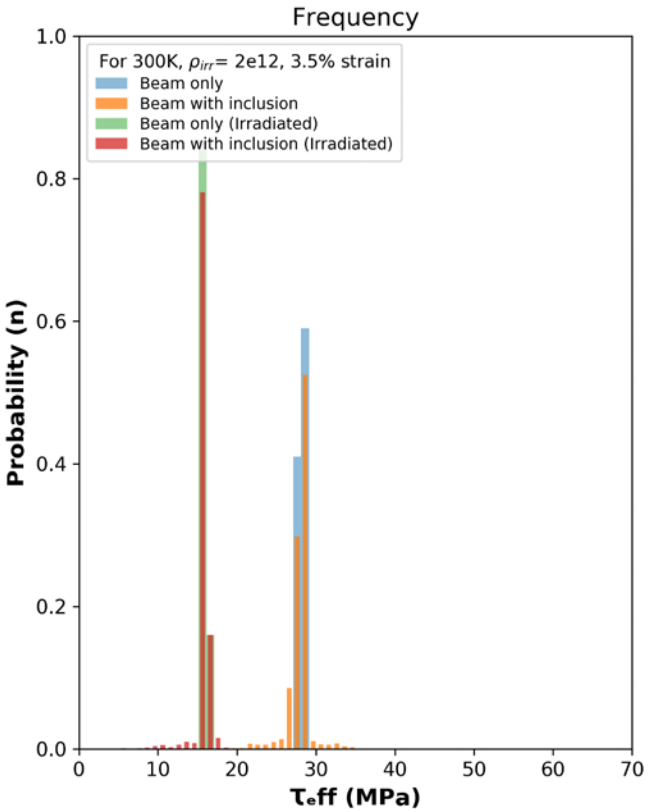

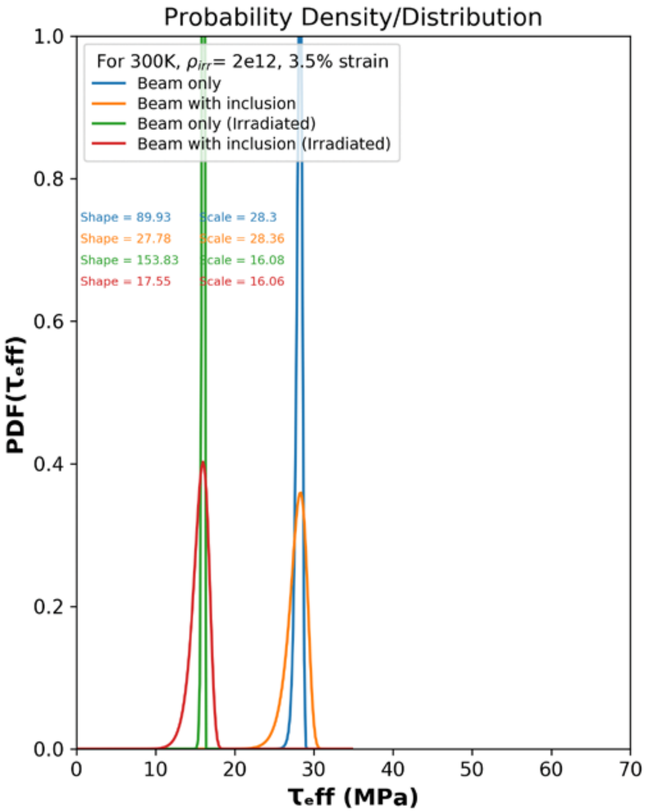

# Preliminary results: dose-dependent stresses

## Irradiation defect size - 15 nm

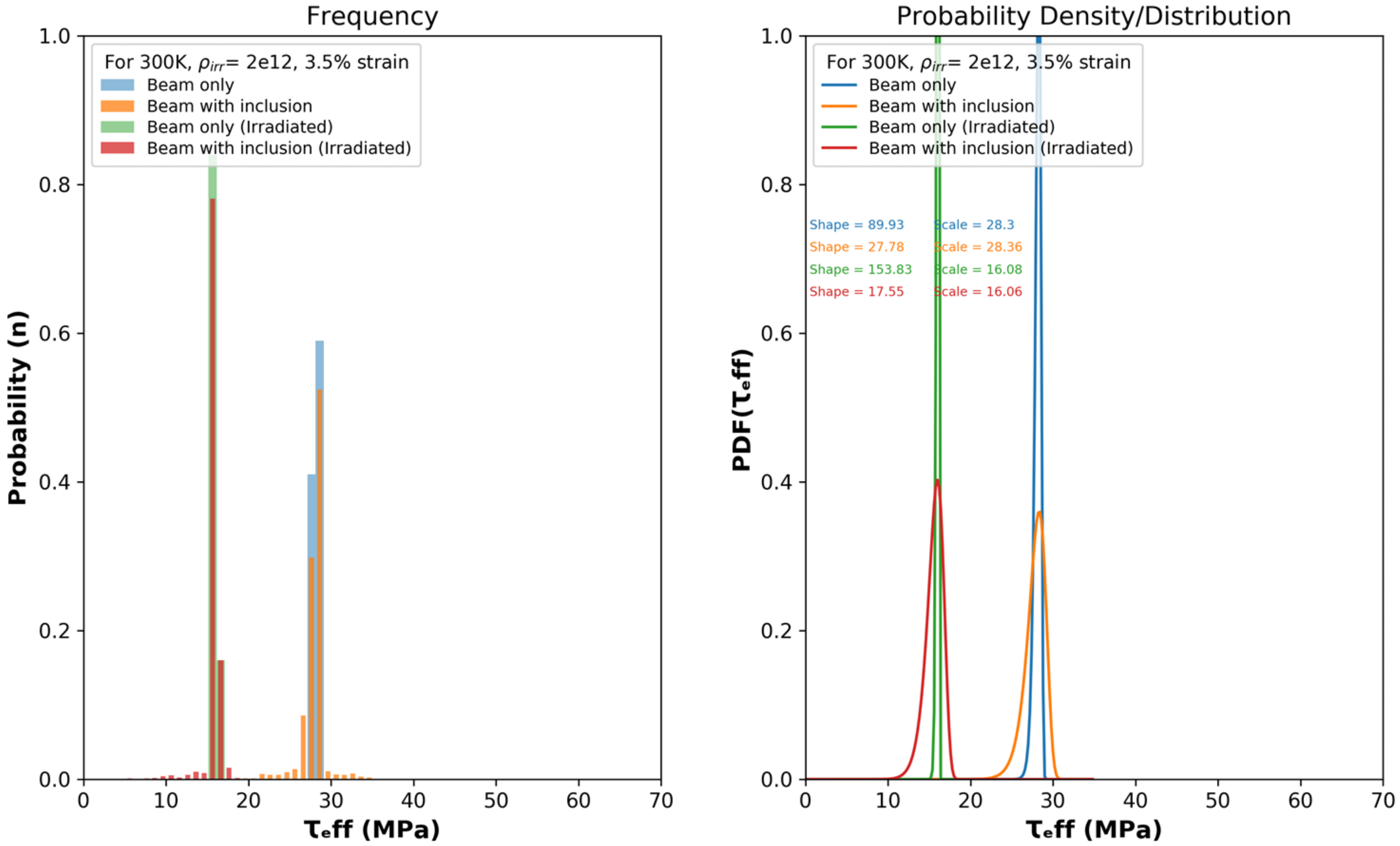

# Preliminary results: link with MIBF model

Ongoing: to compare ΔDIAT and ΔDBTT based on MIBF prediction

RPV steel microstructure
⇒ local stress distribution σ* inside $V_0$.

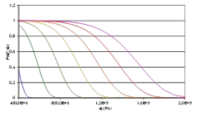

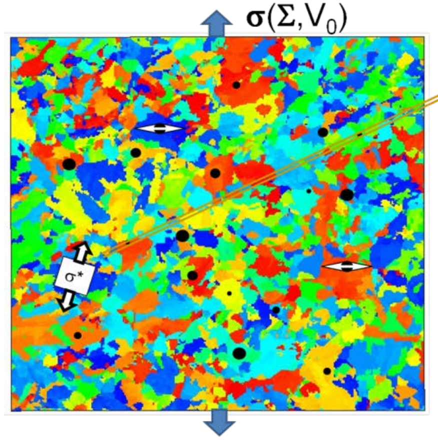

+Δσ or dose-dependent change of Weibull grain stress distribution parameters

$$P_f\left(V_p,\Sigma\right)=1-\exp\left(\int_{V_p}\ln\left(1-P_f\left(V_0,\sigma\right)\right)\frac{dV}{V_0}\right)$$

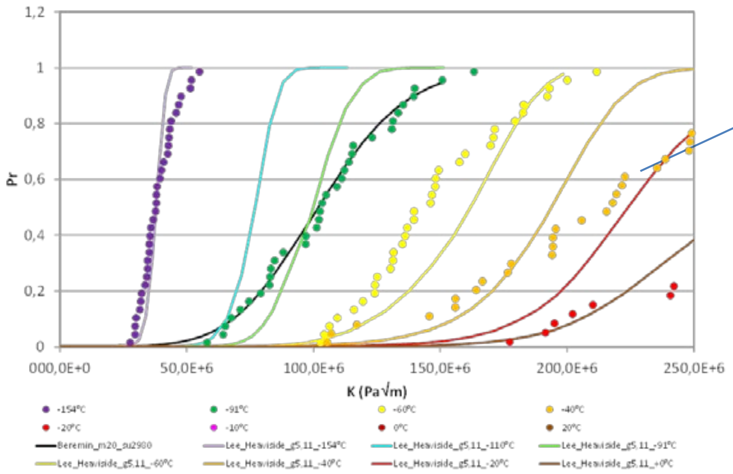

Example: as-received (0 dpa) conditions
Solid line: without grain plasticity
Solid symbols: accounting for grain plasticity

# SUMMARY

In presence of disperse defect populations:

- Weakest link fracture framework: toughness level is controlled by the **plastic zone size «$a_0$»**, off the BF initiators (particles or GB)
- Plastic zone size «$a_0$» is **dose-dependent** and scales with the **apparent (screw) dislocation mobility**
- Apparent dislocation mobility depends on dispersed defect populations and can be estimated using the **statistical ΔDIAT concept**
- Calculated ΔDIAT levels are comparable to DBT transition shifts, for a given disperse defect microstructure ($N$, D)
- DD and ΔDIAT approach used in support of crystal plasticity calculation framework
- Corresponding dose-dependent stress distributions to feed MIBF model, predicting DBT level and shift

Perspectives:

- To apply ΔDIAT method to a broader range of materials and irradiation conditions
- To predict dose-dependent evolutions of upper shelve level

# The SOTERIA Consortium

SOTERIA

DE LA RECHERCHE À L'INDUSTRIE
cea

IRSN
INSTITUT
DE RADIOPROTECTION
ET DE SÛRETÉ NUCLÉAIRE

ÚJV

KTH
VETENSKAP
OCH KONST

ARTS
ET MÉTIERS
ParisTech

eDF

VATTENFALL

UPC
UNIVERSITAT POLITÈCNICA
DE CATALUNYA
BARCELONATECH

grupo
tecnatom

PAUL SCHERRER INSTITUT
PSI

VTT

ARTTIC
INTERNATIONAL MANAGEMENT SERVICES

AREVA

Centrum výzkumu Řež s.r.o.
Research Centre Rez

framatome

MANCHESTER
1824
The University of Manchester

wood.

PHIMECA
Solutions for robust engineering

HZDR
HELMHOLTZ
ZENTRUM DRESDEN
ROSSENDORF

SCK•CEN
STUDIECENTRUM VOOR KERNENERGIE
CENTRE D'ETUDE DE L'ENERGIE NUCLEAIRE

European
Commission

GOBIERNO
DE ESPAÑA

MINISTERIO
DE ECONOMÍA
Y COMPETITIVIDAD

Ciemat
Centro de Investigaciones
Energéticas, Medioambientales
y Tecnológicas

cnrs

Institut "Jožef Stefan", Ljubljana, Slovenija

# The SOTERIA Contacts

**The SOTERIA Project Coordinator**

Christian ROBERTSON
CEA
christian.robertson@cea.fr

**The SOTERIA Project Office**

Herman BERTRAND
ARTTIC
bertrand@arttic.eu

www.soteria-project.eu

This project received funding under the Euratom research and training programme 2014-2018 under grant agreement N° 661913.

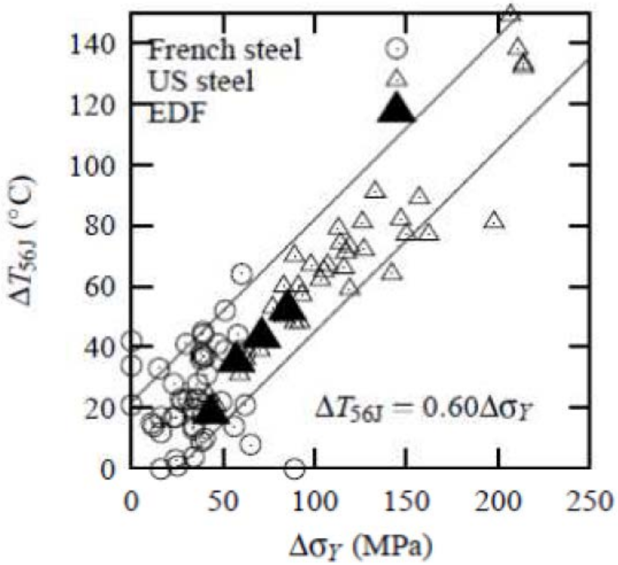

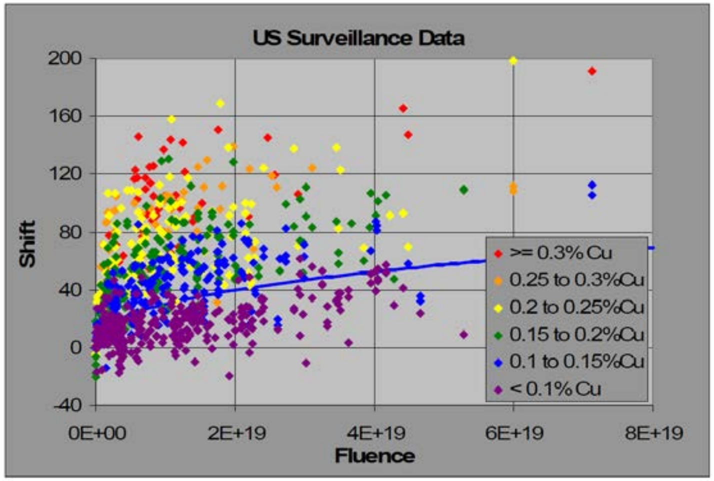

Williams, 2005 (ISQUID)

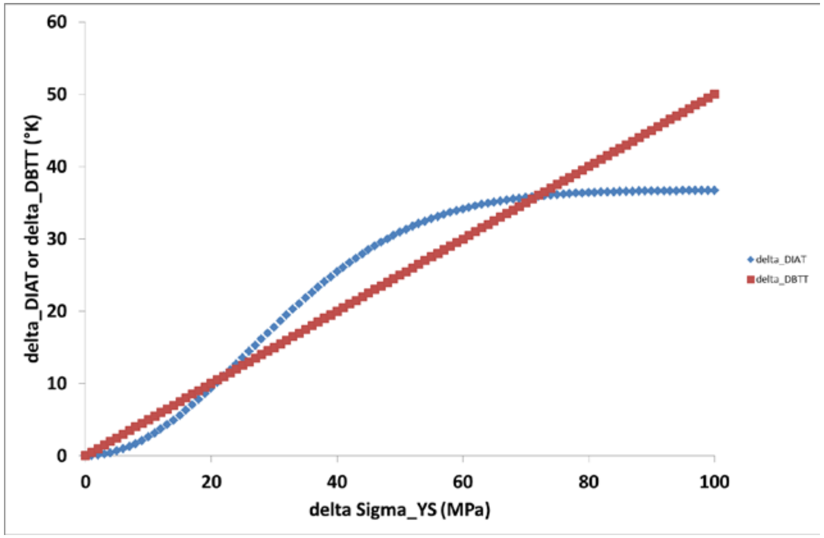

# Fracture toughness in RPV steels?

## RPV steel fracture toughness evolution

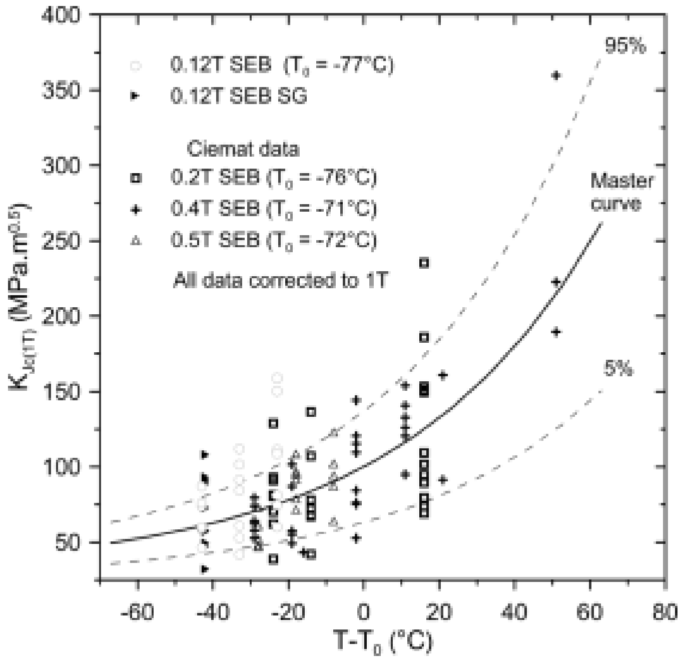

*J. Pressure Vessel Technol* 139(4), 041410 (2017)

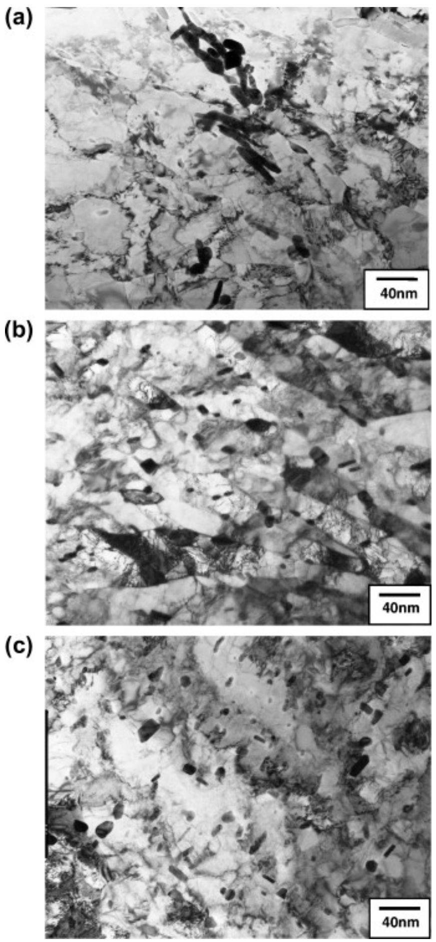

JNM, 407, 2010, Pages 126-135

Low-C
ferritic
RPV steel

- ☞ Populations of inclusions/particles
- ☞ Sub-grain laths and lath-blocks

# Discussion: ΔDIAT concept validation

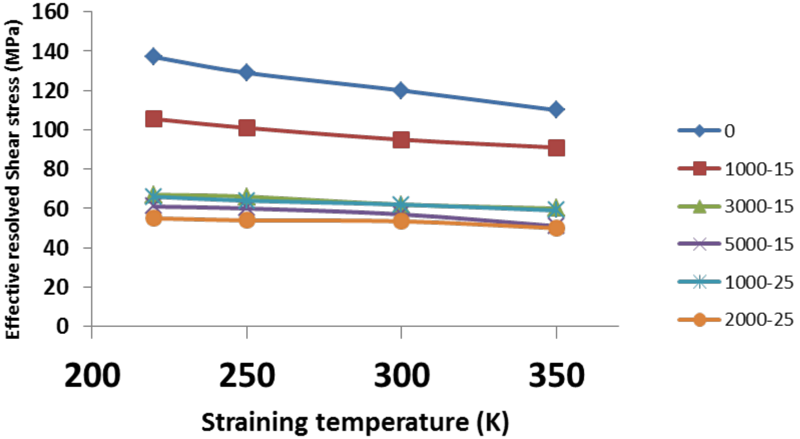

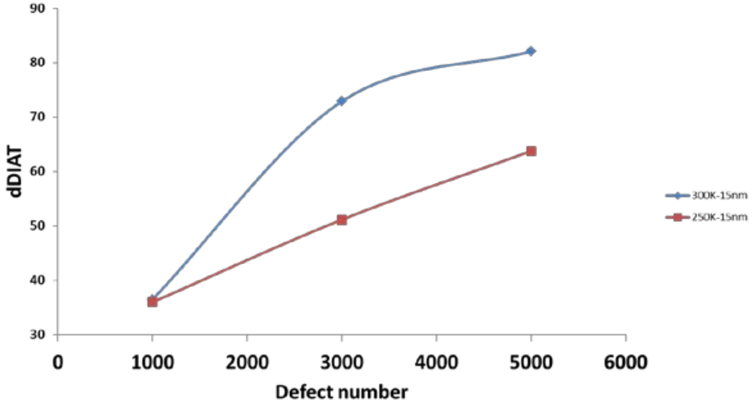

Dose-independent «Master curve»: tau*

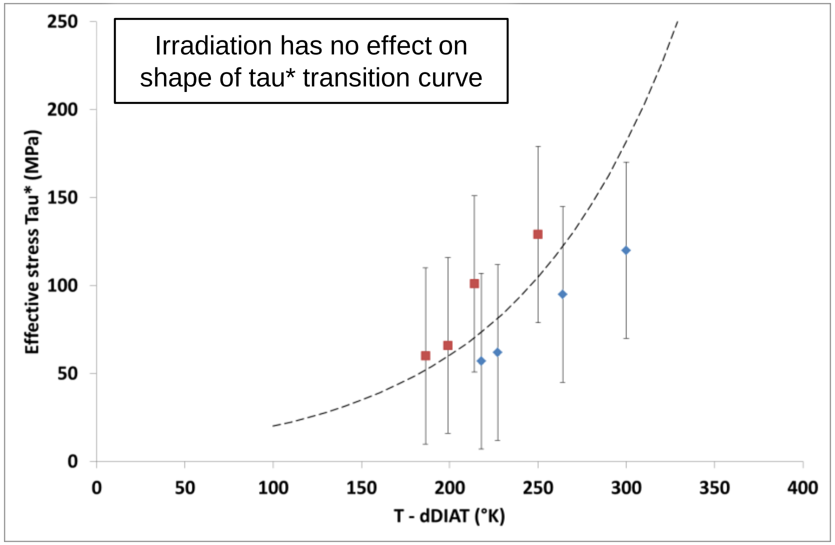
Irradiation has no effect on shape of tau* transition curve

Dose-independent Master curve: K

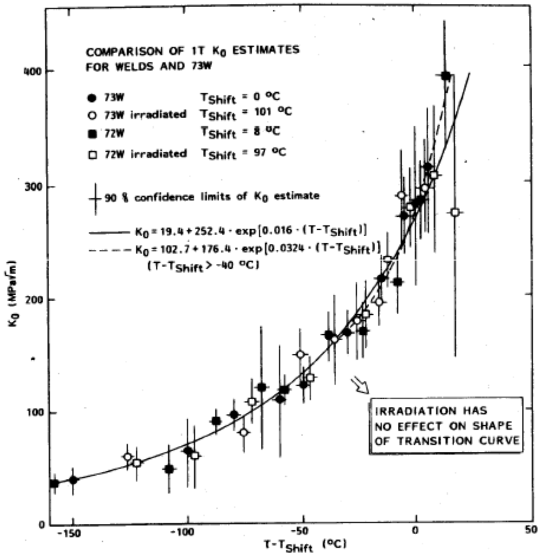
COMPARISON OF 1T $K_0$ ESTIMATES FOR WELDS AND 73W

IRRADIATION HAS NO EFFECT ON SHAPE OF TRANSITION CURVE